



## Efficient polymer-based nanocatalysts with enhanced catalytic performance in wet air oxidation of phenol

Esther M. Sulman<sup>a,\*</sup>, Valentina G. Matveeva<sup>a</sup>, Valentin Yu. Doluda<sup>a</sup>, Alexander I. Sidorov<sup>a</sup>, Natalia V. Lakina<sup>a</sup>, Alexei V. Bykov<sup>a</sup>, Michael G. Sulman<sup>a</sup>, Pyotr M. Valetsky<sup>b</sup>, Leonid M. Kustov<sup>c</sup>, Olga P. Tkachenko<sup>c</sup>, Barry D. Stein<sup>d</sup>, Lyudmila M. Bronstein<sup>e,\*\*</sup>

<sup>a</sup> Tver State Technical University, Department of Biotechnology and Chemistry, 22 A. Nikitina St., 170026 Tver, Russia

<sup>b</sup> A.N. Nesmeyanov Institute of Organoelement Compounds, 28 Vavilov St., Moscow 119991, Russia

<sup>c</sup> N.D. Zelinsky Institute of Organic Chemistry, Leninsky Prospect 47, Moscow 119991, Russia

<sup>d</sup> Indiana University, Department of Biology, Bloomington, IN 47405, USA

<sup>e</sup> Indiana University, Department of Chemistry, 800 E. Kirkwood Av., Bloomington, IN 47405, USA

### ARTICLE INFO

#### Article history:

Received 3 June 2009

Received in revised form 11 September 2009

Accepted 10 November 2009

Available online 17 November 2009

#### Keywords:

Platinum

Nanoparticles

Catalytic wet air oxidation

Phenol

### ABSTRACT

In this paper we report the synthesis of robust and efficient nanocatalysts based on Pt-containing nanoparticles (NPs) formed in the pores of hypercrosslinked polystyrene (HPS) and their catalytic performance in the phenol CWAQ under mild conditions. The Pt species were incorporated in HPS using wet impregnation of platinum acid in tetrahydrofuran followed by  $\text{NaHCO}_3$  treatment. The catalysts containing from 0.11 to 4.85 wt.% of Pt were studied by X-ray fluorescence analysis, transmission electron microscopy, X-ray absorption spectroscopy, X-ray photoelectron spectroscopy, and liquid nitrogen physisorption methods. The NP sizes were found to be independent of the amount of platinum acid used for impregnation, but rather controlled by the pores of HPS. Three types of Pt species: Pt(0), Pt(II), and Pt(IV), constituted the NP composition. The effects of the phenol and catalyst initial concentrations and temperature were investigated in the phenol CWAQ. Removal of 97% of the phenol with 94.2% selectivity to  $\text{CO}_2$  and  $\text{H}_2\text{O}$  were observed for the most active catalyst containing 0.95 wt.% Pt. These parameters are significantly higher than those for the conventional  $\text{Al}_2\text{O}_3$ -Pt catalyst with the similar amount of the active metal or for Pt(5%)/activated carbon.

© 2009 Elsevier B.V. All rights reserved.

### 1. Introduction

The purification of wastewaters from phenol compounds (phenol, chlorophenols, m-, p-, and o-cresols, pyrocatechin, resorcin, etc.) is one of the most essential tasks of environmental catalysis considering the hazardousness of phenols [1–7]. Although numerous methods are known for the elimination of phenols from water [8–10], the majority of them are physical that preserve the phenol mass balance, i.e., lead to the pollutant redistribution/concentration without its transformation to non-hazardous substances. Nowadays there is a large amount of phenols in the environment, hence, novel technologies for the conversion of phenols to non-hazardous or useful substances

should be developed and implemented at the industrial scale [8,11,12]. The ideal purification is a complete oxidation of phenols to  $\text{CO}_2$  and  $\text{H}_2\text{O}$ . (Although  $\text{CO}_2$  is one of the greenhouse gases, it is far less dangerous than initial phenols.) This can be achieved by a microbiological method, but this method is constrained by the high phenol content in wastewaters. The application of chemical non-catalytic methods is limited by high-energy consumption and high-capital costs [11,13–15]. Catalytic conversion is considered to be the best solution to this problem [14–16]. A great challenge in this field, however, is to provide a nearly 100% phenol conversion in mild conditions and thus, the search for the most efficient and selective catalyst is one of the vigorously developing areas of the environmental catalysis [14–17].

The promising methods of dephenolization include catalytic oxidation in supercritical water and  $\text{CO}_2$  (SCWO) [15,18,19] or catalytic wet air oxidation (CWAQ) [20–26]. SCWO is very effective in the decomposition of organic waste without formation of such hazardous compounds (side products) as benzofurans, dioxins, and nitric oxide [15]. The main shortcoming of this method is corrosion

\* Corresponding author. Tel.: +7 4822 449348; fax: +7 4822 449317.

\*\* Corresponding author. Tel.: +1 812 855 3727; fax: +1 812 855 8300.

E-mail addresses: [sulman@online.tver.ru](mailto:sulman@online.tver.ru) (E.M. Sulman), [lybronst@indiana.edu](mailto:lybronst@indiana.edu) (L.M. Bronstein).

and harsh reaction conditions. CWAO allows the sewage treatment at ambient temperatures and pressures. The use of the catalyst accelerates considerably the oxidation rate and reduces waste concentration to the level at which the sewage can be used for technological needs [27–30]. The key to the successful application of the CWAO process is the heterogeneous catalysis due to stability of such catalysts compared to homogeneous or colloidal ones. Platinum and ruthenium metals and cerium, titanium, manganese and iron oxides deposited on zeolites, aluminosilicates, ceria, alumina and different types of carbon have been employed as catalysts [1,4,5,21,23,27,28,31–40], yet the catalysts based on the platinum group metals demonstrated much higher activities. However, all these catalysts use a high content (up to 25 wt.%) of the active metal and they are often unstable due to metal leaching [31,36,39,40]. These problems can be solved by the use of more efficient catalysts requiring less active metal ( $\sim 5$  wt.%) [27,31,32,35], however, the decrease of the amount of the active metal leads to the formation of large amounts of carbon-containing polymers adsorbed on the catalyst surface, which in turn, results in a significant catalyst deactivation [31,36,39].

Platinum deposited on activated carbon (AC) is the mostly studied catalyst in CWAO of phenol [28,37,38,41,42]. Normally, the process is carried out at pH 2–9 in the temperature range 120–250 °C and at the 0.5–2.0 MPa pressure. This results in COD removal of 95% at the 5 wt.% amount of active metal however, again the catalyst is easily deactivated by metal leaching and by formation of carbon-containing film of different composition on the surface of the active metal [28,37,38].

Although nanocatalysts based on nanoparticles (NPs) have been extensively studied in such catalytic reactions as hydrogenation [43,44], coupling [45,46], dehydrosulfurization [47], and oxidation [48–51], only a few studies have recently reported the CWAO of phenolic compounds with metal and metal oxide nanoparticles [52–54]. Among them, iron nanoparticles [52,53] (without support) and nanoclusters of  $\text{SnO}_2$  [54] deposited on the surface of silica nanospheres were used as colloidal solutions. However, the degree of phenol removal with these catalysts did not exceed 70%, while leaching and possibility of multiple uses of the recovered catalysts were not considered. In addition, these systems are technologically irrelevant as they are unstable and coagulate during catalytic reactions, leading to catalyst deactivation.

In the present paper we report on catalytic properties of Pt-containing nanoparticles formed in the pores of hypercrosslinked polystyrene (HPS) in the CWAO of phenol to non-toxic  $\text{CO}_2$  and  $\text{H}_2\text{O}$  (Scheme 1). HPS is the first representative of a new class of crosslinked polymers characterized by unique topology and unusual properties [55,56]. Due to its high crosslinking density, which can exceed 100%, HPS consists of nanosized rigid cavities in

the size range of 2–4 nm. The commercial HPS [57] may contain also large mesopores or even macropores [58]. These polymers have a large inner surface area (usually nearly  $1000\text{--}1500\text{ m}^2\text{ g}^{-1}$ ) and the ability to swell in practically any liquid. All of that makes HPS a promising nanostructured material for nanoparticle formation. The use of analogous catalysts based on HPS and containing Pt, Pd, or Ru species was reported by us earlier in oxidation of L-sorbose [58,59], D-glucose [60], and enantioselective hydrogenation of ethylpyruvate [61]. These catalysts demonstrated high efficacy and stability after multiple catalytic cycles. Recently, we explored such a catalyst containing 4.85 wt.% of Pt in the phenol CWAO [62]. This catalyst yielded the 97% phenol conversion in the CWAO and stable catalytic performance even after several catalytic cycles, but the comparatively high Pt content makes this catalyst unappealing for practical applications. In this paper we report new studies on the influence of the Pt content in HPS in the range 0.11–2.91 wt.% on the catalyst structure and properties in comparison with the catalyst containing 4.85 wt.% Pt [62] in order to determine the lowest limit of the Pt content in HPS-Pt, providing desirable catalytic activity and selectivity. The catalysts studied are comprehensively characterized using X-Ray fluorescence analysis (XFA), transmission electron microscopy (TEM), X-ray absorption spectroscopy (XANES + EXAFS), X-ray photoelectron spectroscopy analysis (XPS), and liquid nitrogen physisorption methods.

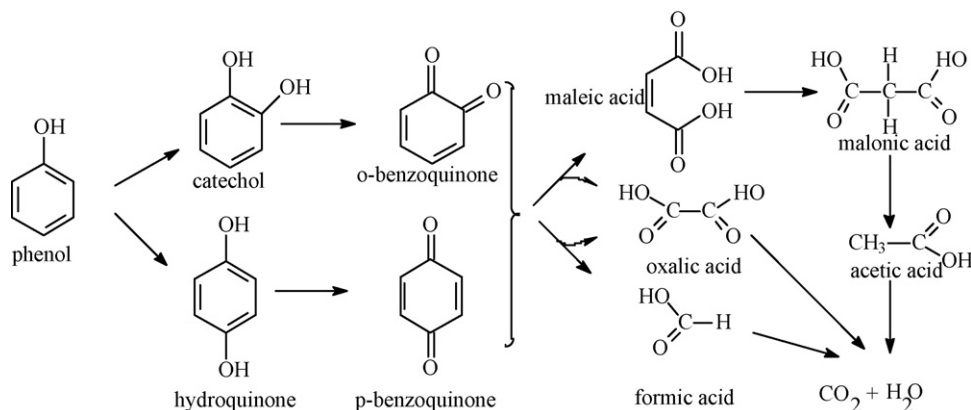
## 2. Materials and methods

### 2.1. Materials

The hypercrosslinked polystyrene, HPS, was purchased from Puroline Int. (UK), as Macronet MN 270/3860 type 2/100 (designated as MN-270). The size of the MN-270 granules is 50–70  $\mu\text{m}$ . The granules were washed with acetone and water twice and dried under vacuum for 24 h. Pt(5%)/AC was purchased from Fluka. Sodium hydrogen carbonate ( $\text{NaHCO}_3$ ), chloroplatinic acid hexahydrate  $\text{H}_2\text{PtCl}_6 \cdot 6\text{H}_2\text{O}$  (platinic acid), reagent-grade THF, sulfuric acid, and phenol were purchased from Sigma–Aldrich and used as received. The conventional catalyst,  $\text{Al}_2\text{O}_3$ –Pt-1%, was supplied by Evonic Ind. Reagent-grade oxygen of 98.4% purity was received from local oxygen purification station. Distilled water was purified with Elsi-Aqua water purification system.

### 2.2. Catalyst synthesis

The catalysts were prepared by impregnation of HPS with platinic acid in a THF solution. In a typical synthesis, 0.4 g of  $\text{H}_2\text{PtCl}_6 \cdot 6\text{H}_2\text{O}$  was dissolved under nitrogen in 7 mL of THF for 60 min stirring. To the platinic acid solution 3 g of HPS was added.



Scheme 1. Reaction pathways of the phenol oxidation.

**Table 1**

Surface areas and pore volumes of HPS and the HPS-Pt catalysts.

Catalyst	NP size, nm	BET surface area, m <sup>2</sup> g <sup>-1</sup>	Mesopore volume, mL g <sup>-1</sup>	Micropore volume, mL g <sup>-1</sup>
HPS	–	1450	0.26	0.47
HPS-Pt-0.11%	2.3 ± 0.4	1386/1380 <sup>a</sup>	0.24/0.25 <sup>a</sup>	0.50/0.52 <sup>a</sup>
HPS-Pt-0.95%	2.3 ± 0.5	1291/1315 <sup>a</sup>	0.19/0.19 <sup>a</sup>	0.48/0.49 <sup>a</sup>
HPS-Pt-2.91%	2.1 ± 0.5	1223/1210 <sup>a</sup>	0.18/0.19 <sup>a</sup>	0.45/0.45 <sup>a</sup>
HPS-Pt-4.85%	2.2 ± 0.4	1177/1190 <sup>a</sup>	0.17/0.17 <sup>a</sup>	0.44/0.47 <sup>a</sup>
Pt(5%)/AC	–	1111	0.76	0.45

<sup>a</sup> After a catalytic test.

The suspension was stirred for 10 min so that the solution was absorbed by the polymer. Then the polymer sample was dried at 75 °C for 1 h. Note that 3 g of HPS used can absorb 12 mL of THF, so 7 mL of the platinum acid solution should be absorbed by the surface layer of the HPS grains. The dried polymer matrix after impregnation with H<sub>2</sub>PtCl<sub>6</sub>·6H<sub>2</sub>O was treated with 5 mL of 0.1 mol L<sup>-1</sup> NaHCO<sub>3</sub> solution to form platinum oxides [63]. The HPS-Pt catalyst was then recovered by filtration, washed with 2 L of water at pH 6.4–7.0 and dried at 75 °C for 12 h. The Pt content was found to be 4.85 wt.% by XFA [62]. This sample is designated as HPS-Pt-4.85%. The samples with different Pt contents (2.91%, 0.95%, and 0.11%) were prepared following the same methodology with 0.24, 0.08, and 0.008 g of H<sub>2</sub>PtCl<sub>6</sub>·6H<sub>2</sub>O and were designated as HPS-Pt-2.91%, HPS-Pt-0.95%, and HPS-Pt-0.11%, respectively (Table 1).

### 2.3. Phenol CWAO

The catalytic wet air oxidation of phenol was conducted batchwise in a PARR 4200 apparatus equipped with a stirrer (maximum 1500 rpm). This apparatus provides independent control over parameters such as phenol or catalyst concentrations, temperature, pure oxygen feed rate, oxygen pressure and stirring rate. It is worth mentioning that for catalytic studies in the phenol CWAO, pure oxygen is used instead of air to exclude the influence of other components of air on the catalyst [2,3,21,64].

A suspension of the catalyst and the aqueous solution of phenol (20 mL) prepared at a predetermined concentration (see Table 1) were placed in the reactor. The rate of the oxygen feed was controlled by a rotameter. The high stirring rates (up to 1500 rpm) were employed here to ensure good mixing without external diffusion limitation. Samples of the reaction mixture were periodically removed for analysis. At the end of each experiment, the catalyst was separated by filtration and the filtrate was analyzed to measure the content of phenol and intermediates using HPLC and chemical oxygen demand (COD) method (see below). The catalyst samples after catalytic tests were washed with distilled water (500 mL total) until pH 6.4–7.0 and dried overnight at 75 °C for BET and TEM evaluation. The catalysts can be repeatedly used, however, without regeneration (washing and drying) in the following catalytic tests.

### 2.4. HPLC analysis

The analysis of phenol and reaction intermediates was performed using a Waters-410 HPLC chromatograph. Ion exchange chromatography using a 250 mm × 4 mm tungsten column characterized by a theoretical plate number of 82,000 was chosen for a sample analysis. Repregel H (7 mkm) served as a stationary phase, whereas 0.5 mol L<sup>-1</sup> sulfuric acid was used as the mobile phase. The flow rate was held constant at 0.5 mL min<sup>-1</sup> at 70 bar and 20 °C. The refractometer detector and conductometer were used for component detection. The concentrations of phenol and detected intermediates were determined using external standards.

### 2.5. Chemical oxygen demand analysis

The liquid samples were also immediately analyzed for the remaining organic compounds by COD method using the closed reflux colorimetric method [65], according to which the organic substances are oxidized (digested) by potassium dichromate K<sub>2</sub>Cr<sub>2</sub>O<sub>7</sub> at 160 °C in a sealed tube. When orange colored Cr<sub>2</sub>O<sub>7</sub><sup>2-</sup> is reduced, green colored Cr<sup>3+</sup> is formed which can be detected in a spectrophotometer set at 600 nm. The relation between absorbance and COD concentration is established by calibration with standard solutions of potassium hydrogen phthalate, in the range of COD values between 50 and 1200 mg/L.

### 2.6. X-ray fluorescence analysis

The Pt content was determined by XFA measurements performed with a Spectroscan – Maks – GF1E spectrometer (Spectron, St-Petersburg, Russia) equipped with Mo anode, LiF crystal analyzer and SZ detector. The analyses were based on the Co Kα line. A series of HPS/Pt standards was prepared by mixing 1 g of HPS with 10–20 mg of standard Pt compounds.

### 2.7. Liquid nitrogen physisorption

Nitrogen physisorption was conducted at the normal boiling point of liquid nitrogen using a Beckman Coulter SA 3100 apparatus (Coulter Corporation, Miami, Florida). Prior to the analysis, samples were degassed in a Becman Coulter SA-PREP apparatus for sample preparation (COULTER CORPORATION, Miami, Florida) at 120 °C in vacuum for 1 h.

### 2.8. TEM analysis

Transmission electron microscopy was performed with a JEOL JEM1010 transmission electron microscope operated at accelerating voltage of 80 kV. Pt-containing HPS grains were ground with a mortar and a pestle in liquid nitrogen. Powders were embedded in epoxy resin and subsequently microtomed at ambient temperature. Images of the resulting thin sections (ca. 50 nm thick) were collected with the Gatan digital camera. Particle size analysis was performed using the Scion Image Processing Toolkit and the Adobe Photoshop software package for background bleaching.

### 2.9. X-ray absorption spectroscopy (XANES + EXAFS)

Pt L<sub>3</sub> XAS measurements were carried out on the beamline X1 (DESY, Hamburg) (Pt L<sub>3</sub>-edge, 11564 eV) using a double-crystal Si(1 1 1) monochromator, which was detuned to 50% of maximum intensity to exclude higher harmonics in the X-ray beam. The spectrum of metal Pt-foil was recorded simultaneously between 2nd and 3rd ionization chambers for energy calibration. Platinum reference spectra were recorded using standard reference compounds with different electronic state (Pt(0)-foil, Pt(II)Cl<sub>2</sub> and Pt(IV)O<sub>2</sub>). The spectra were collected in the transmission mode at

$T = 80$  K in order to decrease the Debye–Waller factors. In the XANES region, the spectra had a constant step of the photon energy 0.5 eV and in the EXAFS region, the constant step of the wave vector of photoelectrons was equal to  $0.025 \text{ \AA}^{-1}$ . All experiments were performed using an *in situ* EXAFS cell in which a small amount of the grained sample was exposed at room temperature to the flowing He. Analysis of the EXAFS spectra was performed with the software VIPER for Windows [66].

### 2.10. X-ray photoelectron spectroscopy analysis

XPS data were obtained using Mg K $\alpha$  ( $h\nu = 1253.6$  eV) radiation with a ES-2403 spectrometer modified with an analyzer PHOIBOS 100 produced by SPECS (Germany). All the data were acquired at an X-ray power of 200 W and an energy step of 0.1 eV. Samples were allowed to outgas for 180 min before analysis and were sufficiently stable during the examination. Data analysis was performed by CasaXPS.

## 3. Results and discussion

### 3.1. The structure of the HPS-Pt samples: TEM, $N_2$ physisorption, and XPS

In order to comprehensively characterize the HPS-Pt catalysts, we used several techniques allowing us to obtain information on both polymeric matrix and Pt species. As we know from our preceding work [58,59–62], the impregnation of HPS with platonic acid in THF leads to formation of Pt compound NPs. Fig. 1 presents TEM images of the HPS samples containing 2.91, 0.95, and 0.11 wt.% Pt. The TEM image of HPS-Pt-4.85% is presented in our preceding paper [62]. The mean NP sizes for all the samples (Table 1) are nearly the same, indicating that the NP size is independent of the platonic acid concentration in the THF solution, revealing that HPS controls the NP formation. Therefore, at the different Pt contents, the different amount of NPs should form.

The BET surface areas and volumes of micropores and mesopores of HPS and the HPS-Pt catalysts are presented in Table 1. These data demonstrate that the increase of the Pt content leads to a decrease of both the surface area and mesopore volume. At the same time, micropore volume first slightly increases (for HPS-Pt-

0.11%) and then slightly decreases (for HPS-Pt-4.85%). The former effect can be explained by creation of the small amount of micropores due to the location of NPs in mesopores (i.e., due to the space between the particles and mesopore walls), while the latter effect is due to blockage of some micropores at the higher Pt content. Both these effects can annihilate each other's influence for the intermediate Pt contents.

The pore size distributions are presented in Fig. 2. Parent HPS contains small mesopores ( $\leq 4$  nm) which are responsible for 22% of the mesopore volume and larger mesopores (5–50 nm), the volume of which measures 78%. The presence of larger mesopores is crucial for catalytic performance because it favors the transport of the reactants toward the active sites [58,60,61], while small mesopores accommodate NPs. This is confirmed by the broadening of the mesopore volume distributions along with their shift to smaller mesopore sizes (see inset in Fig. 2). We believe that NP formation occurs in small mesopores ( $\leq 4$  nm) (Fig. 2) because they provide a stronger retention of the platonic acid solution due to capillary condensation: the smaller the pores, the stronger the capillary retention of the adsorbing molecules [67]. For larger mesopores, reversible multilayer adsorption takes place followed by desorption under solvent evaporation, thus nanoparticles do not form there.

It is noteworthy that Pt(5%)/AC used for comparison with the HPS-based catalysts has similar amount of micropores (Table 1), but much larger amount of mesopores (10% of small mesopores and 90% of large mesopores) and even macropores ( $> 50$  nm).

It is worth mentioning that the Pt-containing NP size (2.1–2.3 nm, see above) is noticeably lower than the pore size. On the other hand, this NP size is constant for all the samples therefore it is controlled by the small mesopores. The shrinkage of the compound NPs compared to the pore size can be explained by oxidation of Pt species (see below), leading to denser NPs (oxides are denser than metal complexes). In addition these NPs can be surrounded by organic ligands (products of THF oxidation [59]) and/or by  $\text{NaHCO}_3$  or its reaction products, adding the layer to the particles which is not registered by TEM. The survey XPS spectra show the presence of oxygen, carbon, platinum, chlorine, and sodium in all the samples (Table 2), corroborating this hypothesis. It is noteworthy that due to poor compatibility of the hydrophobic HPS walls and comparatively polar NPs, a near-wall space between the HPS walls and NPs can be created as well, determining the smaller NP size.

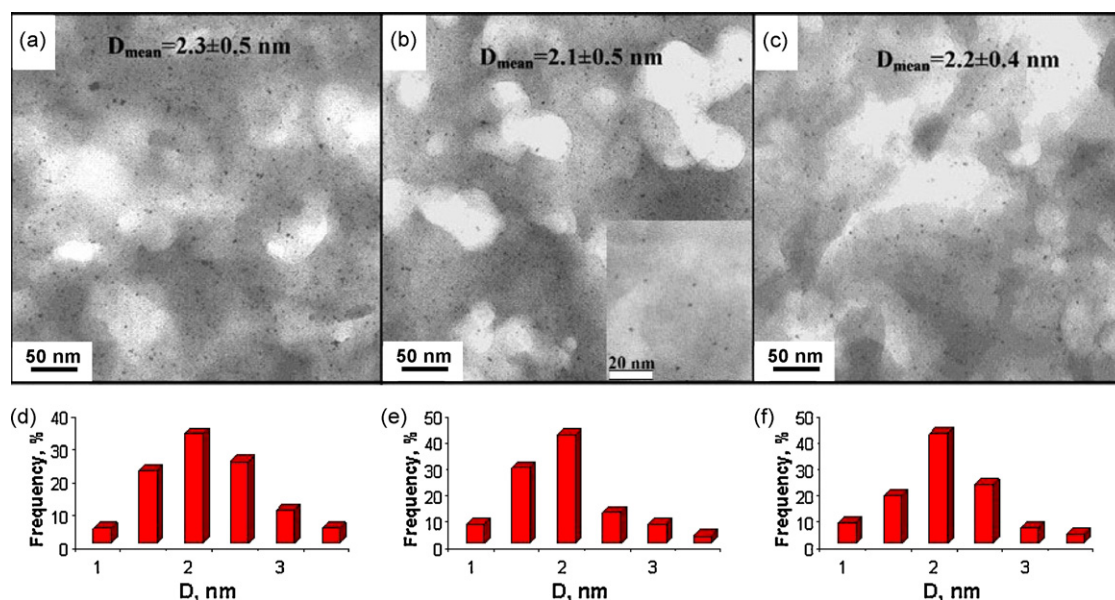


**Fig. 1.** TEM images and their histograms of the HPS-Pt samples with 2.91 wt.% (a and d), 0.95 wt.% (b and e) and 0.11 wt.% (c and f) Pt (c). Inset in (b) shows a higher magnification image.

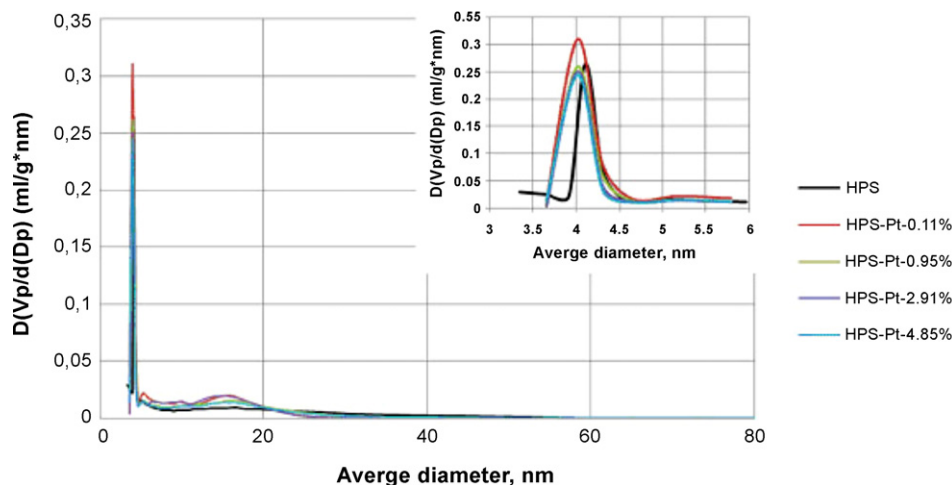


Fig. 2. Dependence of the pore volume vs. pore diameter for HPS and the HPS-Pt catalysts.

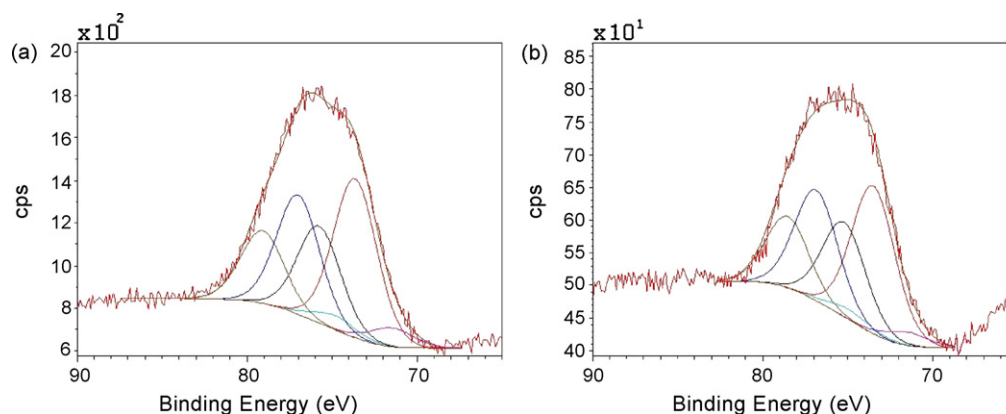


Fig. 3. High resolution XPS spectra (red lines) of HPS-Pt-2.91% (a) and HPS-Pt-0.95% (b) in the Pt 4f region and their deconvolution curves. (For interpretation of the references to color in the figure caption, the reader is referred to the web version of the article.)

The composition of the Pt-containing NPs was analyzed with XPS. In our preceding papers [58,59] we demonstrated that Pt(IV) is partially reduced to Pt(II) or even Pt(0) due to oxidation of THF in the presence of water. For the samples discussed here, the deconvolution of the high resolution XPS Pt spectra (Fig. 3, Table 3) results in three components for each HPS-Pt sample, the Pt 4f<sub>7/2</sub> energy of which (71.5, 73.6–73.7, 75.7–75.8 eV) can be ascribed to Pt(0), Pt(II), and Pt(IV) species, while their ratio depends on the Pt content. (The spectrum for HPS-Pt-0.11% was not well resolved and is not shown, while the high resolution XPS spectrum for HPS-Pt-4.85% is reported in Ref. [62].) For comparison, the tabulated Pt 4f<sub>7/2</sub> binding energy ranges for Na<sub>2</sub>PtCl<sub>6</sub>, Na<sub>2</sub>PtCl<sub>4</sub>, and Pt(0) are 75.5–75.8, 72.8–73.6, and 71.0–71.5 eV, respectively. In all the samples, except HPS-Pt-4.85%, amount of Pt(II) species prevails while the amount of the Pt(0) species varies with the lowest (1.9 at.%) in HPS-Pt-4.85%. It is noteworthy that the HPS-Pt sample

(1.72 wt.% Pt) obtained in our preceding work [58] using similar impregnation with platinum acid in THF, but without the NaHCO<sub>3</sub> treatment, contains 25.9 at.% Pt(0), 48.3 at.% Pt(II), and 25.8 at.% Pt(IV), i.e., much higher fraction of reduced species, suggesting that the NaHCO<sub>3</sub> treatment indeed allows for a higher fraction of oxidized species due to formation of platinum oxides with high solubility products which should ensure high stability of the catalysts. Considering that in all the samples both Pt(II) and Pt(IV) are present, we believe that mixed PtO<sub>2</sub>·2PtO and pure PtO<sub>2</sub>·H<sub>2</sub>O may form [63,68,69]. Presence of chlorine in the samples (Table 2) may suggest formation of PtCl<sub>2</sub> or NaCl or a remainder of platinum acid (our spectra do not allow us to distinguish between these compounds). Thus, according to XPS the NPs, which are observed in

Table 2

The elemental content in the HPS-Pt catalysts obtained from the XPS survey spectra<sup>a</sup>.

Catalyst	Pt, at.% (wt.%) <sup>b</sup>	Cl, at.%,	C, at.%,	O, at.%,	Na, at.%,
HPS-Pt-4.85%	2.5 (26.7)	1.3	71.7	18.7	5.8
HPS-Pt-2.91%	0.8 (10.3)	0.7	69.7	20.4	8.4
HPS-Pt-0.95%	0.2 (2.8)	1.0	68.7	21.7	8.4

<sup>a</sup> The data for the HPS-Pt-0.11% sample is not shown because of a poor signal-to-noise ratio for the Pt and Cl peaks.

<sup>b</sup> For Pt, the weight percentage is shown along with a traditional atomic percentage for easy comparison with the XFA data.

Table 3

Characteristics of the Pt-containing HPS by XPS.

Catalyst notation	Pt species	( $E \pm 0.1$ ) Pt 4f <sub>7/2</sub> (eV)	Pt content, at.%, before (after) oxidation
HPS-Pt-4.85%	Pt(0)	71.5 $\pm$ 0.2	1.9 (2.3)
	Pt(II)	73.6 $\pm$ 0.2	48.3 (50.2)
	Pt(IV)	75.7 $\pm$ 0.2	51.7 (47.5)
PS-Pt-2.91%	Pt(0)	71.5 $\pm$ 0.2	6.9 (7.7)
	Pt(II)	73.6 $\pm$ 0.2	57.9 (60.8)
	Pt(IV)	75.8 $\pm$ 0.2	35.2 (31.5)
HPS-Pt-0.95%	Pt(0)	71.5 $\pm$ 0.2	5.2 (6.5)
	Pt(II)	73.7 $\pm$ 0.2	57.8 (61.4)
	Pt(IV)	75.7 $\pm$ 0.2	37.0 (32.1)

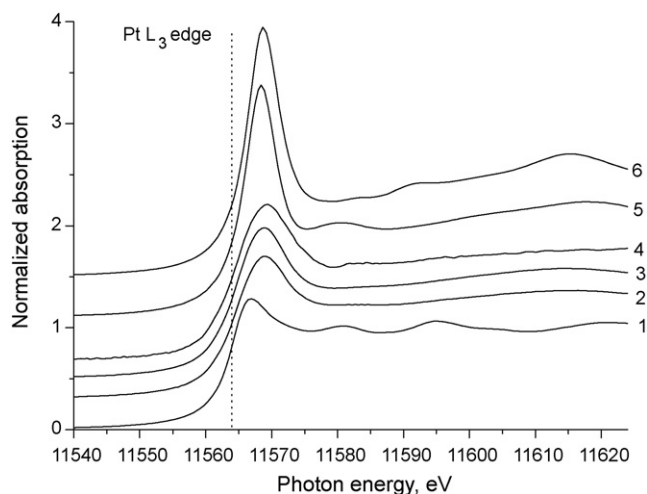


**Fig. 4.** XANES spectra of Pt(0)-foil (1), HPS-Pt-4.85% (2), HPS-Pt-2.91% (3), HPS-Pt-0.95% (4), Pt(IV)O<sub>2</sub> (5), and Pt(II)Cl<sub>2</sub> (6).

the TEM images of all the samples, are of a mixed composition including Pt(0), Pt(II), and Pt(IV) species.

### 3.2. The structure of the HPS-Pt samples: XANES and EXAFS

Further confirmation of the mixed composition of the Pt-containing NPs was obtained from XANES and EXAFS. Fig. 4 shows the Pt L<sub>3</sub> XANES spectra of the HPS-Pt catalysts with Pt contents 4.85, 2.91, and 0.95 wt.% and the platinum references. HPS-Pt-0.11% was not analyzed because of the low Pt content. There is a small negative shift of the position of the Pt 2p<sub>3/2</sub> X-ray absorption relative to the L<sub>3</sub>-edge corresponding to that of Pt(IV)O<sub>2</sub> and Pt(II)Cl<sub>2</sub> and a positive shift relative to that of Pt(0)-foil in the spectra of the catalysts. A comparison of the XANES spectra belonging to the catalysts indicates that the Pt electronic state in HPS-Pt samples is different from that of individual Pt(0), Pt(II), and Pt(IV) species. Moreover, the intensity of the white line in the spectra of the HPS-Pt catalysts is almost double compared with that of Pt(0)-foil and, at the same time, only one third of that of both Pt(II)Cl<sub>2</sub> and Pt(IV)O<sub>2</sub>.

The nature of these differences can be clarified using the EXAFS data. The Fourier transformation (FT) EXAFS spectra of HPS-Pt-4.85% and HPS-Pt-2.91% are shown in Fig. 5. The EXAFS spectrum of

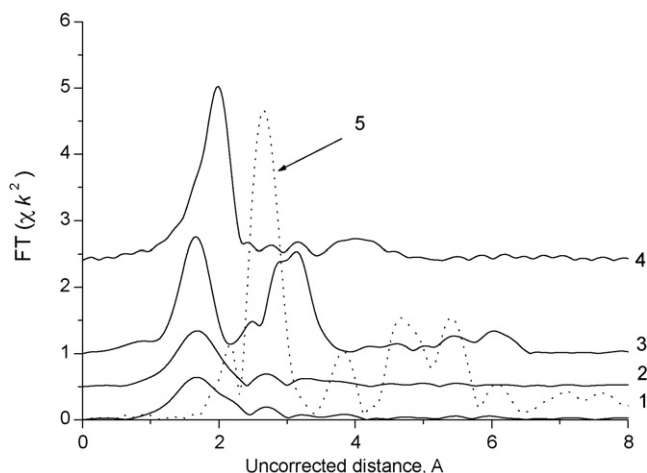


**Fig. 5.** EXAFS spectra of HPS-Pt-4.85% (1), HPS-Pt-2.91% (2), Pt(IV)O<sub>2</sub> (3), Pt(II)Cl<sub>2</sub> (4), and Pt(0)-foil (5).

HPS-Pt-0.95% had a low signal-to-noise ratio and was not analyzed. A comparison of the EXAFS spectra of HPS-Pt-4.85% and HPS-Pt-2.91% shows that the local structure of Pt species in these samples is different from that in Pt(0)-foil, Pt(II)Cl<sub>2</sub>, and Pt(IV)O<sub>2</sub>, while it is very similar between the two HPS-Pt samples. The position of the first peak in the EXAFS spectra of the HPS-Pt samples is similar to that in Pt(IV)O<sub>2</sub>, indicating that there are oxygen atoms in the first coordination shell of the Pt atoms in HPS-Pt-4.85% and HPS-Pt-2.91%. However, the intensity of the scattering events in the EXAFS spectra of the HPS-Pt samples from the nearest neighbors of the Pt atom is low, revealing that in the HPS-Pt catalysts Pt has fewer neighbors (lower coordination number). The first peak in the EXAFS spectra of the HPS-Pt catalysts is significantly broadened, indicating the presence of the second shell of the Pt atoms. The shoulder on this peak can be observed, the position of which is similar to that in Pt(II)Cl<sub>2</sub>, indicating that there are chlorine atoms in the second coordination shell of the Pt atoms in both HPS-Pt-4.85% and HPS-Pt-2.91% samples. The position of the second peak in the EXAFS spectra of HPS-Pt samples is similar to that of the Pt(0)-foil spectrum, but of much lower intensity.

The Pt L<sub>3</sub> EXAFS spectra of HPS-Pt samples may be readily fitted in both (*k* and *r*) spaces with a three-shell model: one oxygen, one chlorine and one platinum shell around the central absorbing platinum atom. The example of fitting is shown in Fig. 6. The results of the model fits are given in Table 4.

The average Pt–O distance in the first coordination shell in the HPS-Pt samples ( $2.049 \div 2.053 \pm 0.004$  Å) is longer than that of PtO<sub>2</sub> (2.003 Å). The average Pt–O coordination number ( $3.0 \div 3.3 \pm 0.1$ ) is smaller than that of bulk PtO<sub>2</sub> (4.0). The average Pt–Cl distance in the second shell in the HPS-Pt samples ( $2.394 \div 2.404 \pm 0.008$  Å) is longer than that of PtCl<sub>2</sub> (2.311  $\div$  2.318 Å). The average Pt–Cl coordination number ( $0.6 \div 1.2 \pm 0.2$ ) is smaller than that of bulk PtCl<sub>2</sub> (4.0). The average Pt–Pt distance in the second coordination shell in the HPS-Pt samples ( $2.937 \div 2.943 \pm 0.002$  Å) is shorter than that of PtO<sub>2</sub> (3.136  $\div$  3.184 Å) and longer than that of Pt-foil (2.772 Å). The average Pt–Pt coordination number ( $0.9 \div 1.7 \pm 0.2 \div 0.3$ ) is smaller than that of bulk PtO<sub>2</sub> (4.0) and Pt(0)-foil (12.0). These results indicate that platinum in the HPS-Pt samples exists in both cationic, Pt(II) and Pt(IV), and metallic, Pt(0), states.

Thus, the results obtained from X-ray absorption spectroscopy (bulk sensitive method) confirm the data of XPS (surface sensitive method), indicating that platinum in the HPS-Pt samples exists as a mixture of different electronic state (0, II and IV). Moreover from the EXAFS spectra of the HPS-Pt samples one can see that the intensity of the second peak (2.69 Å uncorrected distance) is higher in HPS-Pt-2.91% than in HPS-Pt-4.85%. The fit results of the EXAFS spectra (Table 4) confirm that the Pt–Pt coordination number is double in HPS-Pt-2.91% compared to that of HPS-Pt-4.85%, also indicating the higher Pt(0) content in the former sample, which is in a good agreement with the XPS data.

At the same time the EXAFS data show that the Cl/Pt atomic ratio in the bulk of HPS-Pt-4.85% sample is 1.2 (0.52 by XPS) and in the bulk of HPS-Pt-2.91% sample is 0.6 (0.875 by XPS). This result indicates the nonuniform distribution of the residual chlorine atoms in these two catalysts.

### 3.3. The performance of the HPS-Pt catalysts in CWAO

To investigate the catalytic performance of these catalysts in phenol CWAO, we varied reaction conditions such as the phenol concentration in the range *C*<sub>0</sub> 0.04–0.44 mol(phenol)/L, and the temperature in the range 50–95 °C. The other reaction conditions (Table 5) were kept constant. In order to evaluate the NP stability after the phenol CWAO, we studied the catalysts using TEM. After five catalytic cycles only insignificant NP aggregation was observed (Fig. 7) leading to the mean NP diameters of  $2.3 \pm 0.4$ ,  $2.1 \pm 0.5$ , and

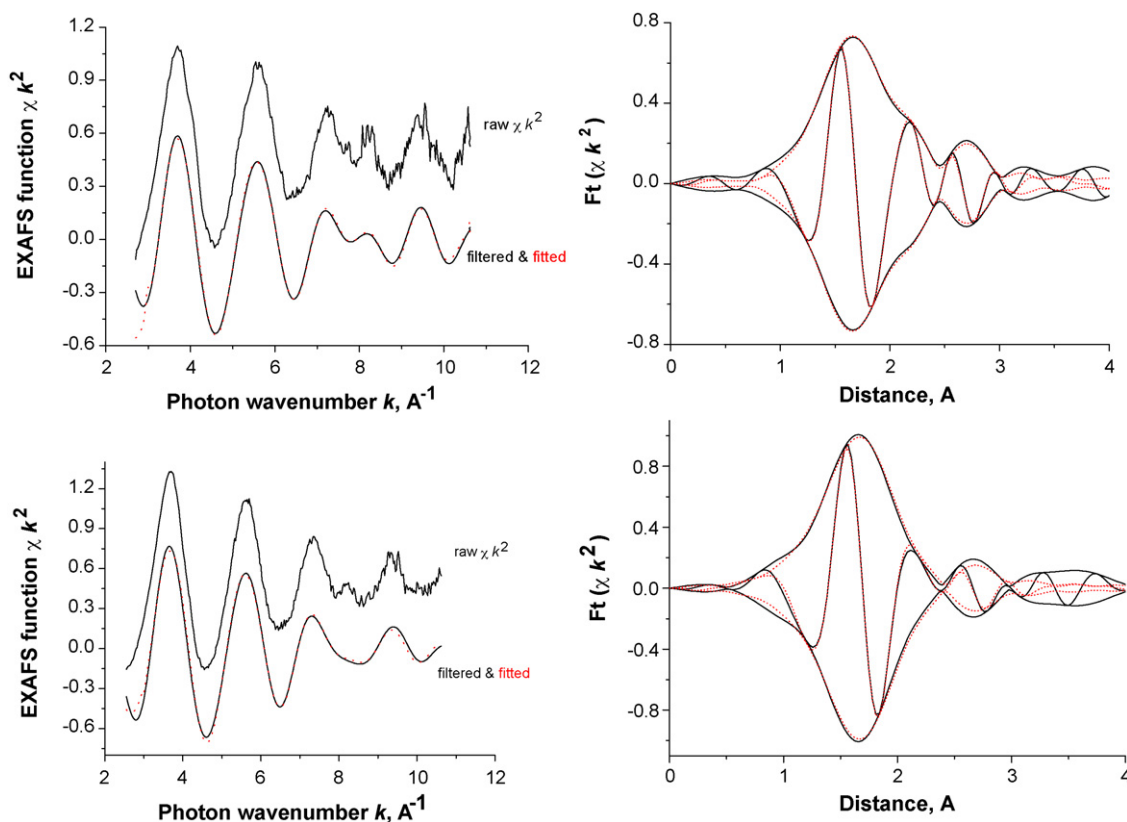


Fig. 6. Model fits of the Pt L<sub>3</sub> EXAFS spectra of the HPS-Pt-4.85% (top) and HPS-Pt-2.91% (bottom) samples in k-space (left) and r-space (right).

2.3 ± 0.5 nm for HPS-Pt-2.91%, HPS-Pt-0.95%, and HPS-Pt-0.11%, respectively. Thus, the NP morphology remains practically unchanged after the catalytic reaction. XPS data presented in Table 2 also demonstrate only insignificant changes of the oxidation state of the Pt species: the Pt(0) and Pt(II) contents slightly increase, while the Pt(IV) content slightly decreases, revealing that the Pt species are becoming slightly more reduced.

As a criterion allowing evaluation of the dependence of phenol conversion on time at various phenol ( $C_0$ ) and catalyst ( $C_c$ ) concentrations, the ratio  $q = C_0/C_c$  (mol/mol) was used. The

**Table 4**  
The EXAFS data for the HPS-Pt catalysts.

Sample	Path	$r$ (Å)	CN	$\sigma^2 \times 10^{-3}$ Å <sup>2</sup>	$\Delta E$ (eV)
HPS-Pt-4.85%	Pt–O	2.049 ± 0.004	3.0 ± 0.1	10 ± 1	24 ± 1
	Pt–Cl	2.394 ± 0.008	1.2 ± 0.2	10 ± 1	–33 ± 1
	Pt–Pt	2.937 ± 0.002	0.9 ± 0.3	6 ± 1	–18 ± 1
HPS-Pt-2.91%	Pt–O	2.053 ± 0.004	3.3 ± 0.1	11 ± 1	24 ± 1
	Pt–Cl	2.404 ± 0.008	0.6 ± 0.2	13 ± 1	–33 ± 1
	Pt–Pt	2.943 ± 0.002	1.7 ± 0.2	9 ± 1	–15 ± 1

**Table 5**  
Catalytic activity and selectivity of the catalysts at optimal conditions<sup>a</sup> in the phenol CWAQ.

Catalyst	Conversion of phenol, %	TOF mol(Phen)/ (mol Pt s)	COD removal, %	$E_a$ kJ/mol
HPS-Pt-4.85%	65	$1.6 \times 10^{-3}$	54.3	61 ± 4
HPS-Pt-2.91%	86	$4.6 \times 10^{-3}$	64.1	65 ± 4
HPS-Pt-0.95%	97	$7.3 \times 10^{-3}$	94.2	58 ± 4
HPS-Pt-0.11%	91	$5.8 \times 10^{-3}$	85.4	61 ± 4
Al <sub>2</sub> O <sub>3</sub> –Pt-1%	83	$2.8 \times 10^{-3}$	53.6	72 ± 4
Pt(5%)/AC	61	$1.2 \times 10^{-3}$	57.8	69 ± 4

<sup>a</sup> Reaction conditions: the catalyst concentration ( $C_c$ ) of  $5.15 \times 10^{-3}$  mol(Pt)/L, phenol concentration ( $C_0$ ) of 0.44 mol(phenol)/L, temperature of 95 °C, pressure of 0.1 MPa, time of 5 h, and the oxygen flow rate of 0.018 m<sup>3</sup> h<sup>–1</sup>.

analysis of the primary experimental data, presented in Fig. 8, shows that the higher the  $C_0/C_c$  ratio, the higher the oxidation time, which is typical for most catalytic reactions. The conversion, selectivity (COD removal), and reaction rate (as a turnover frequency, TOF) calculated from the experimental data, are presented in Table 5. With the decrease of the Pt content from 4.85 to 0.95 wt.% the above parameters increase, while the further decrease of the Pt content to 0.11 wt.% leads to their decrease. Thus, the highest conversion, TOF, and selectivity are obtained for HPS-Pt-0.95%. Please note that all catalytic parameters for the HPS-Pt-0.95% catalyst are significantly higher than those for the conventional Al<sub>2</sub>O<sub>3</sub>–Pt-1% catalyst with the similar amount of the active metal or Pt(5%)/AC (Table 5).

The dependence of the concentrations of intermediate products (*p*-benzoquinone, *o*-benzoquinone, maleic acid, and acetic acid) in the phenol CWAQ (Scheme 1) on the reaction time are shown in Fig. 9 for the most active HPS-Pt-0.95% catalyst. As can be seen, the concentration of the intermediates first increases and then decreases, demonstrating that the phenol oxidation with the given catalyst proceeds through several stages before a complete oxidation to CO<sub>2</sub> and H<sub>2</sub>O.

In order to interrogate the influence of the temperature on the catalyst activity and selectivity of all the catalysts and to determine the activation energy in the phenol CWAQ, we varied the reaction temperature in the range 50–95 °C, while other conditions were kept the same (see the footnote to Table 5). An increase of the reaction temperature from 50 to 95 °C leads to the increase of the reaction rate (TOF) and selectivity (COD removal) to CO<sub>2</sub> and H<sub>2</sub>O (Fig. 10). The values of the apparent activation energy calculated from the Arrhenius equation are presented in Table 5. For all the HPS-Pt catalysts, the activation energy is practically the same and noticeably lower than that of the conventional catalyst. The dependence of the phenol conversion and selectivity on time and the selectivity and TOF on temperature are summarized in Fig. 10.

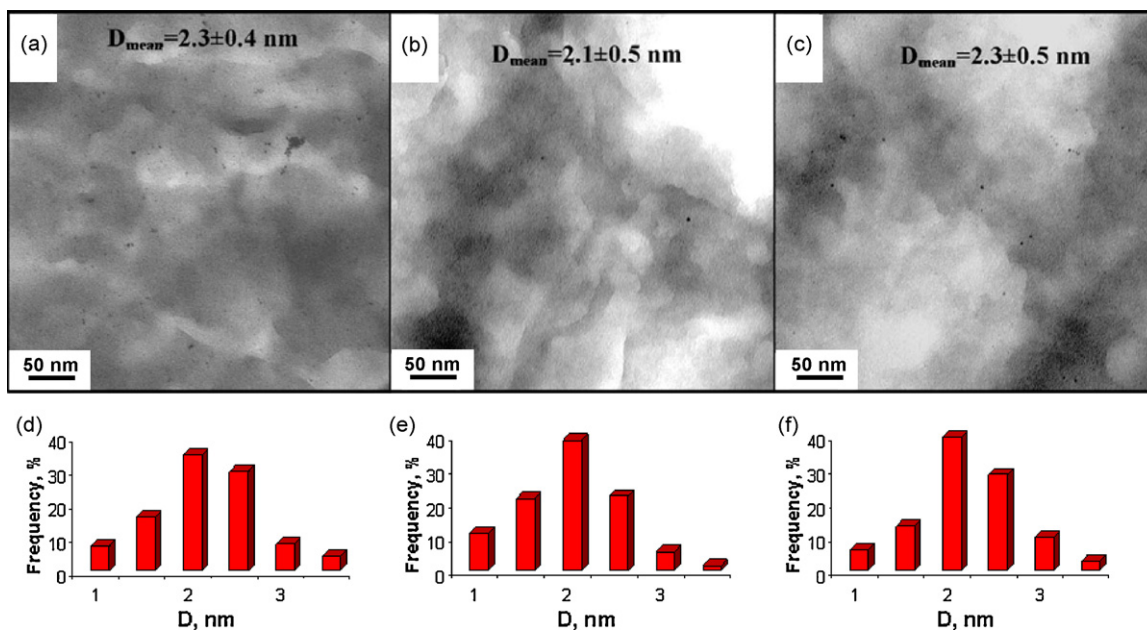


Fig. 7. TEM images and their histograms of the HPS-Pt samples with 2.91 wt.% (a and d), 0.95 wt.% (b and e) and 0.11 wt.% (c and f) Pt after one catalytic test.

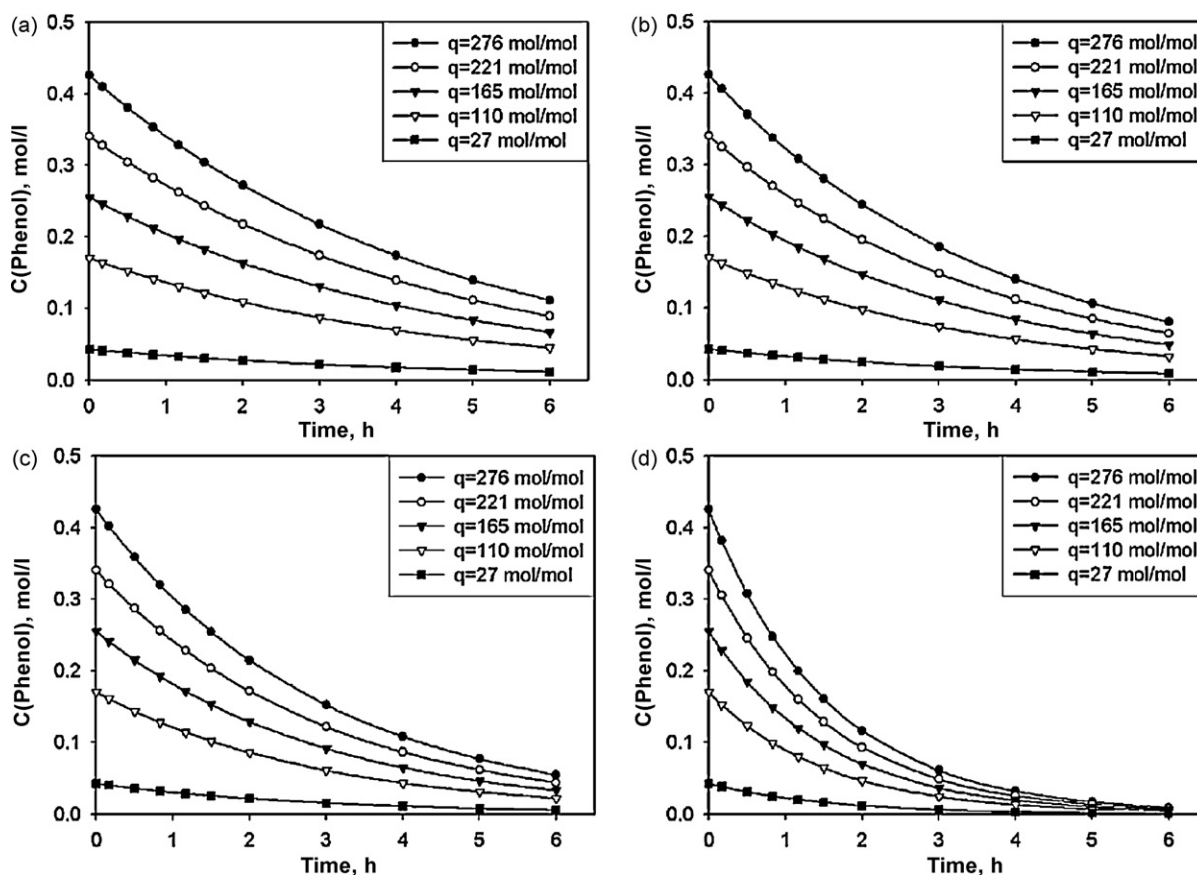


Fig. 8. Dependence of the phenol concentration on time for HPS-Pt-4.85% (a), HPS-Pt-2.91% (b), HPS-Pt-0.95% (c), and HPS-Pt-0.11% (d) (see Table 5 for the reaction conditions).

As can be seen from the data presented in this paper, the worst catalytic properties are observed for the catalyst with the highest Pt content (4.85 wt.% Pt), while the best catalytic performance was found for HPS-Pt-0.95%. Considering that the NP size and Pt composition are nearly the same in all the samples, the differences

in catalytic performance can be ascribed to the different amounts of NPs in the HPS pores. When the Pt content is high, the NPs shield each other as is demonstrated in Scheme 2a. When the Pt content is lower, the NP surface is more readily available for reactants and catalytic performance improves (Scheme 2b). At a very low Pt

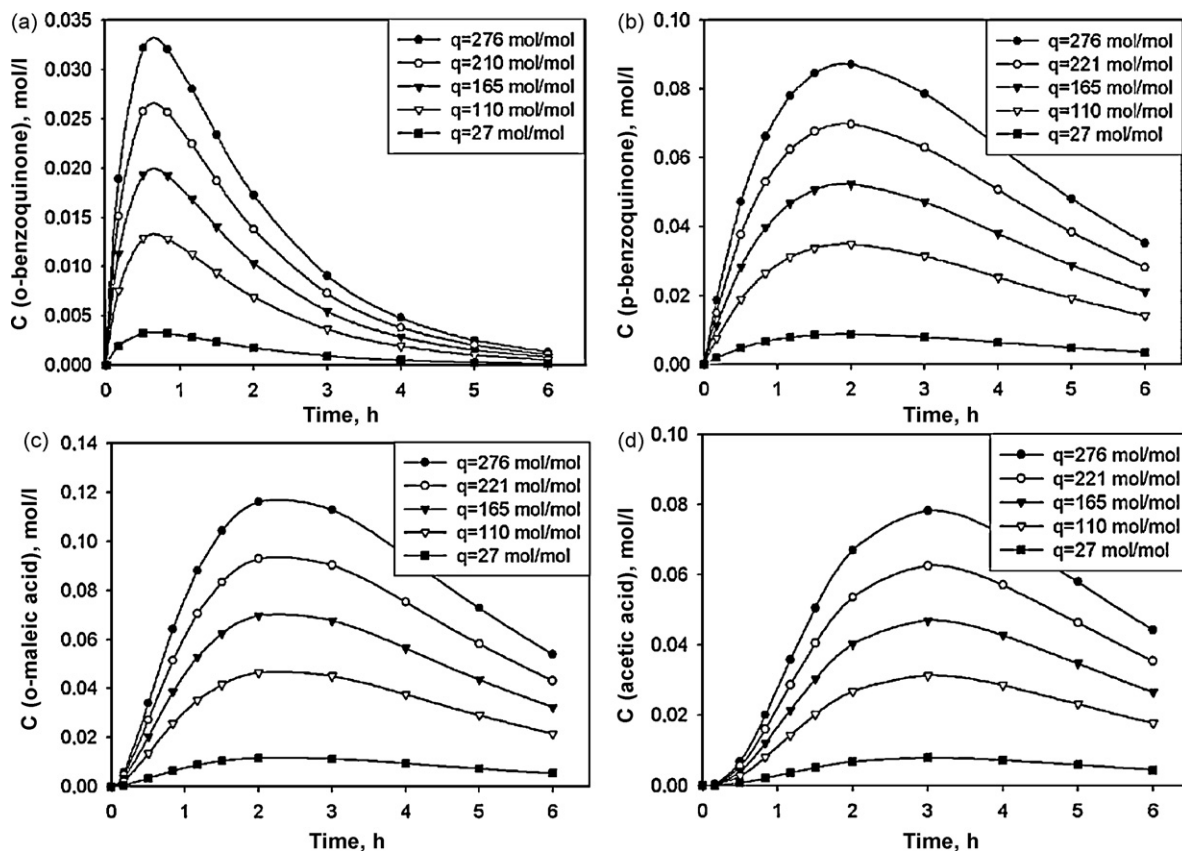


Fig. 9. Dependence of the p-benzoquinone (a), o-benzoquinone (b), maleic acid (c), and acetic acid (d) concentrations on time at different  $q$  values for HPS-Pt-0.95% (see Table 5 for the reaction conditions).

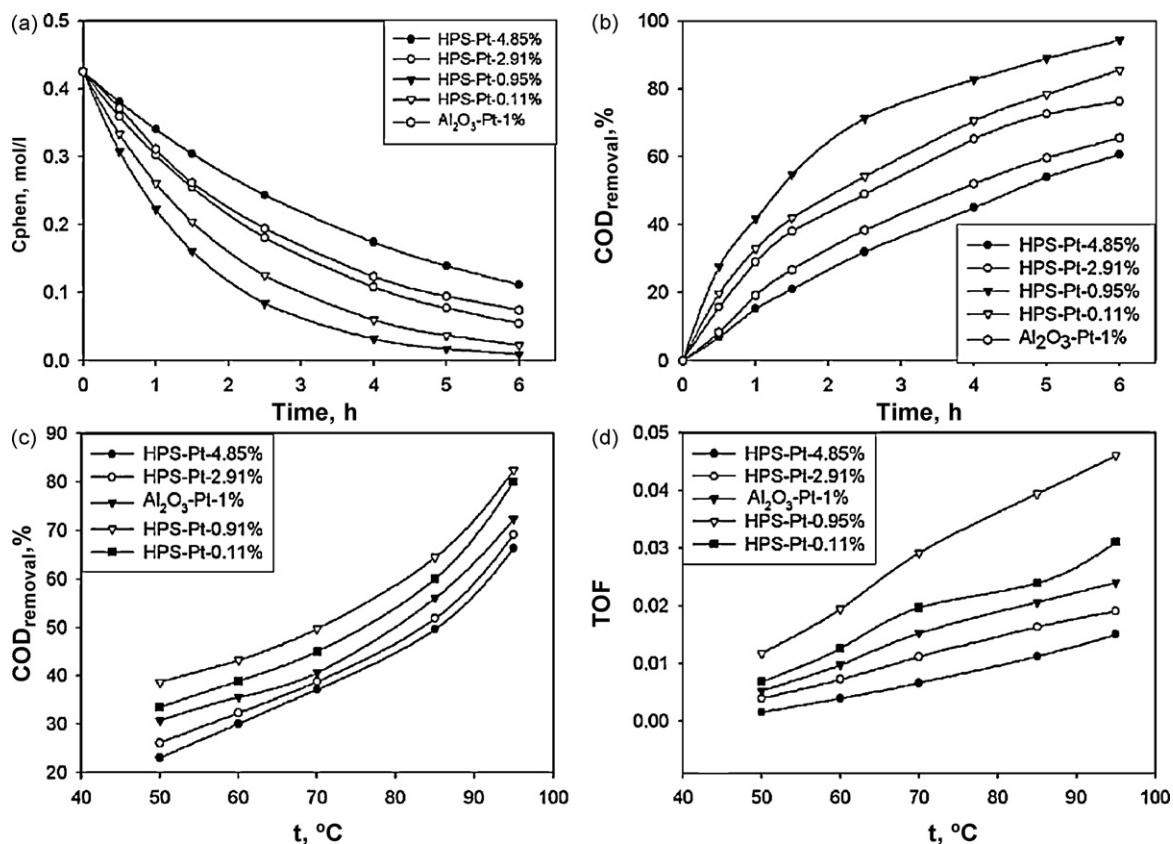
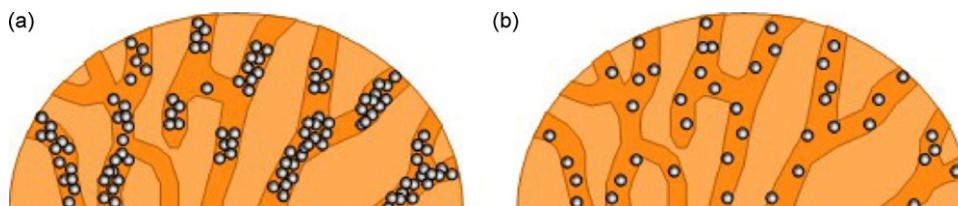


Fig. 10. Dependence of the phenol concentration (a) and COD removal (b) on time and COD removal (c) and TOF (d) on temperature for the HPS-Pt catalysts in comparison with  $Al_2O_3$ -Pt-1% (see Table 5 for the reaction conditions).



**Scheme 2.** Schematic representation of the HPS-Pt catalysts with 4.85 wt.% (a) and 0.95 wt.% (b) Pt.

**Table 6**

Catalytic stability of HPS-Pt-0.95% at optimal conditions<sup>a</sup>.

Amount of catalytic tests	TOF mol(Phen)/(mol Me s)	COD removal, %
1	$7.3 \times 10^{-3}$	94.2
2	$7.1 \times 10^{-3}$	94.4
3	$7.2 \times 10^{-3}$	94.3
4	$7.3 \times 10^{-3}$	94.2
5	$7.2 \times 10^{-3}$	94.3

<sup>a</sup> See Table 5 for reaction conditions.

content (HPS-Pt-0.11%), the amount of Pt seems to be insufficient to provide needed catalytic sites. Comparison of HPS-based catalysts with Pt(5%)/AC shows that despite Pt(5%)/AC contains macropores and a higher amount of large mesopores (Table 1) (the large pores should facilitate the reagent transport and normally lead to the increase of the catalytic activity [58]), the crucial factor in determining the higher catalytic activity is the formation of well-defined ~2 nm NPs which do not aggregate and do not shield each other (Fig. 1b).

The catalytic stability, i.e., the ability of the same catalyst batch to be used multiple times, is a key parameter for industrial applications. Table 6 presents the stability study of the most active and selective catalyst, HPS-Pt-0.95%, during five consecutive catalytic tests. One can see that neither activity nor selectivity (COD removal) changes during the five catalytic tests, revealing high stability of the catalyst synthesized.

#### 4. Conclusions

In this paper we demonstrated that wet impregnation of HPS with platinumic acid in THF followed by the NaHCO<sub>3</sub> treatment leads to the formation of mixed Pt-containing NPs, the sizes of which are independent of the amount of incorporated Pt species and measure about 2.1–2.3 nm. The Pt species include Pt(0), Pt(II), and Pt(IV), the ratio of which varies insignificantly. Despite the similar NP sizes and composition, the catalysts containing different amount of Pt display very different catalytic properties in the phenol CWAQ. The highest conversion, activity, and selectivity, markedly exceeding those of the conventional Al<sub>2</sub>O<sub>3</sub>-Pt-1% with the same amount of Pt or Pt(5%)/AC, were obtained for the HPS-based catalyst containing only 0.95 wt.% Pt, while the catalyst containing 4.85 wt.% Pt is least active and selective. These differences are explained by the shielding of the catalytic sites when the Pt load is too high. The catalysts reported here also display high stability making them promising candidates for environmentally sound catalytic applications.

#### Acknowledgments

We sincerely thank the NATO Science for Peace programme (SfP 981438) for the financial support. Authors also thank HASYLAB (DESY, Germany) for X-ray beam time (project I-20060224 EC).

#### References

- [1] M. Abecassis-Wolfovich, M.V. Landau, A. Brenner, M. Herskowitz, *Ind. Eng. Chem. Res.* 43 (2004) 5089.
- [2] A. Quintanilla, J.A. Casas, J.A. Zazo, A.F. Mohedano, J.J. Rodrigues, *Appl. Catal. B: Environ.* (2006) 115–120.
- [3] A. Santos, P. Yustos, B. Durban, F. Garcia-Ochoa, *Catal. Today* 66 (2001) 511–517.
- [4] I.-P. Chen, S.-S. Lin, C.-H. Wang, L. Chang, J.-S. Chang, *Appl. Catal.* 50 (2004) 49.
- [5] L. Chang, I.-P. Chen, S.-S. Lin, *Chemosphere* 58 (2005) 485.
- [6] S. Kim, S. Ihm, *Top. Catal.* 33 (2005) 171–179.
- [7] Z.P.G. Masende, B.F.M. Kuster, K.J. Ptasinski, F.J.J.G. Janssen, J.H.Y. Katima, J.C. Schouten, *Catal. Today* 79–80 (2003) 357–370.
- [8] K. Takaki, Y. Shimazaki, T. Shishido, K. Takehira, *Bull. Chem. Soc. Jpn.* 75 (2002) 311.
- [9] G.A. Jueptner, *A Method for Wastewater Treatment*, 2004, p. 17.
- [10] W.-W. Sai, *Method to Remove Sulfur Compounds and Aromatic Compounds from Oils for High Octane Gasoline*, 2004.
- [11] D. Yang, M.-K. Wong, Z. Yan, *J. Org. Chem.* 65 (2000) 4179.
- [12] H. Nishino, H. Satoh, M. Yamashita, K. Kurosawa, *J. Chem. Soc., Perkin Trans. 2* (1999) 1919.
- [13] M.M. Hashemi, Y.A. Beni, *J. Chem. Res., Synopses* (1998) 138.
- [14] A. Schmid, F. Hollmann, B. Buehler, *Enz. Catal. Org. Synth.* (2002) 1170.
- [15] F. d'Acunzo, C. Galli, B. Masci, *Eur. J. Biochem.* 269 (2002) 5330.
- [16] P.A. Ganeshpure, A. Sudalai, S. Satish, *Tetrahedron Lett.* 30 (1989) 5929.
- [17] A. Inglot, *Pol. J. Chem.* 60 (1986) 841.
- [18] J.R. Katzer, H.H. Ficke, A. Sadana, *J. Water Pollut. Control. Fed.* 48 (1976) 920.
- [19] W. Kokubo, Y. Oshima, S. Koda, *J. Supercrit. Fluids* 30 (2004) 225.
- [20] F. Mizukami, K. Satoh, S. Niwa, T. Tsuchiya, K. Shimizu, J. Imamura, *Sekiyu Gakkaishi* 28 (1985) 293.
- [21] F. Luck, *Catal. Today* 53 (1999) 81.
- [22] D. Scholz, *Sci. Pharm.* 50 (1982) 78.
- [23] S.K. Mohapatra, F. Hussain, P. Selvam, *Catal. Commun.* 4 (2003) 57.
- [24] M.E. Suarez-Ojeda, A. Fabregat, F. Stueber, A. Fortuny, J. Carrera, *J. Font, Chem. Eng. J.* 132 (2007) 105–115.
- [25] A. Eftaxias, J. Font, A. Fortuny, A. Fabregat, F. Stueber, *Appl. Catal. B: Environ.* 67 (2006) 12–23.
- [26] F. Stuber, I. Polaert, H. Delmas, J. Font, A. Fortuny, A. Fabregat, *J. Chem. Technol. Biotechnol.* 76 (2001) 743–751.
- [27] J. Garcia, H.T. Gomes, P. Serp, P. Kalck, J.L. Figueiredo, J.L. Faria, *J. Hazard. Mater.* 159 (2008) 420–426.
- [28] H.T. Gomes, J.L. Figueiredo, J.L. Faria, *J. Catal. Today* 124 (2007) 254–259.
- [29] T. Cordero, J. Rodriguez-Mirasol, J. Bedia, S. Gomis, P. Yustos, F. Garcia-Ochoa, A. Santos, *Appl. Catal. B: Environ.* 81 (2008) 122–131.
- [30] A. Santos, P. Yustos, S. Rodriguez, F. Garcia-Ochoa, *Appl. Catal. B: Environ.* 65 (2006) 269–281.
- [31] S. Yang, Y. Feng, W. Cai, W. Zhu, Z. Jiang, J. Wan, *Rare Met.* 23 (2004) 131.
- [32] A. Cybulski, J. Trawczynski, *Appl. Catal.* 47 (2004) 1–13.
- [33] D.P. Minh, G. Aubert, P. Gallezot, M. Besson, *Appl. Catal. B: Environ.* 73 (2007) 227–235.
- [34] D.P. Minh, P. Gallezot, M. Besson, *Appl. Catal. B: Environ.* 75 (2007) 71–77.
- [35] N.M. Dobrynkin, M.V. Batygina, A.S. Noskov, P.G. Tsyrulnikov, D.A. Shlyapin, V.V. Schegolev, D.A. Astrova, B.M. Laskin, *Top. Catal.* 33 (2005) 69–76.
- [36] P. Massa, F. Ivorra, P. Haure, R. Fenoglio, *Catal. Lett.* 101 (2005) 201–209.
- [37] Z.P.G. Masende, B.F.M. Kuster, K.J. Ptasinski, F.J.J.G. Janssen, J.H.Y. Katima, J.C. Schouten, *Top. Catal.* 33 (2005) 87–99.
- [38] Z.P.G. Masende, B.F.M. Kuster, K.J. Ptasinski, F.J.J.G. Janssen, J.H.Y. Katima, J.C. Schouten, *Catal. Today* 79 (2003) 357–370.
- [39] J.J. Barbier, L. Olivero, B. Renard, D. Duprez, *Top. Catal.* 33 (2005) 77–86.
- [40] S. Nouisir, S. Keav, J.J. Barbier, M. Bensitel, R. Brahmi, D. Duprez, *Appl. Catal. B: Environ.* 84 (2008) 723–731.
- [41] S. Cao, G. Chen, X. Hu, P.L. Yue, *Catal. Today* 88 (2003) 37–47.
- [42] F. Stuber, J. Font, A. Fortuny, C. Bengoa, A. Eftaxias, A. Fabregat, *Top. Catal.* 33 (2005) 3–50.
- [43] M. Murata, Y. Tanaka, T. Mizugaki, K. Ebitani, K. Kaneda, *Chem. Lett.* 34 (2005) 272.
- [44] M. Ohde, H. Ohde, C.M. Wai, *Langmuir* 21 (2005) 1738.
- [45] C. Xue, G. Arumugam, K. Palaniappan, S.A. Hackney, H. Liu, J. Liu, *Chem. Commun.* (2005) 1055.
- [46] Y. Na, S. Park, S.B. Han, H. Han, S. Ko, S. Chang, *J. Am. Chem. Soc.* 126 (2004) 250.
- [47] N.A. Dhas, K.S. Suslick, *J. Am. Chem. Soc.* 127 (2005) 2368.
- [48] M.S. Wong, I.E. Wachs, W.V. Knowles, *Supported Catalysts Using Nanoparticles as the Support Material*, 2005.

- [49] S. Kim, B.K. Yoo, K. Chun, W. Kang, J. Choo, M.-S. Gong, S.-W. Joo, J. Mol. Catal. A: Chem. 226 (2005) 231.
- [50] J. Shen, W. Shan, Y. Zhang, J. Du, H. Xu, K. Fan, W. Shen, Y. Tang, Chem. Commun. (2004) 2880.
- [51] H. Wang, Z. Jusys, R.J. Behm, J. Phys. Chem. B 108 (2004) 19413.
- [52] S.H. Joo, A.J. Feitz, T.D. Waite, Environ. Sci. Technol. 38 (2004) 2242.
- [53] S.H. Joo, A.J. Feitz, D.L. Sedlak, T.D. Waite, Environ. Sci. Technol. 39 (2005) 1263.
- [54] J.L. Gole, Z.L. Wang, Nano Lett. 1 (2001) 449.
- [55] V.A. Davankov, M.P. Tsyurupa, React. Polym. 13 (1990) 27.
- [56] M.P. Tsyurupa, V.A. Davankov, J. Polym. Sci.: Polym. Chem. Ed. 18 (1980) 1399.
- [57] G. Centi, S. Perathoner, T. Torre, M.G. Verduna, Catal. Today 55 (2000) 61.
- [58] L.M. Bronstein, G. Goerigk, M. Kostylev, M. Pink, I.A. Khotina, P.M. Valetsky, V.G. Matveeva, E.M. Sulman, M.G. Sulman, A.V. Bykov, N.V. Lakina, R.J. Spontak, J. Phys. Chem. B 108 (2004) 18234–18242.
- [59] S.N. Sidorov, I.V. Volkov, V.A. Davankov, M.P. Tsyurupa, P.M. Valetsky, L.M. Bronstein, R. Karlinsey, J.W. Zwanziger, V.G. Matveeva, E.M. Sulman, N.V. Lakina, E.A. Wilder, R.J. Spontak, J. Am. Chem. Soc. 123 (2001) 10502.
- [60] E. Sulman, V. Doluda, S. Dzwigaj, E. Marceau, L. Kustov, O. Tkachenko, A. Bykov, V. Matveeva, M. Sulman, N. Lakina, J. Mol. Catal. A: Chem. 278 (2007) 112–119.
- [61] A. Bykov, V. Matveeva, M. Sulman, P. Valetsky, O. Tkachenko, L. Kustov, L. Bronstein, E. Sulman, Catal. Today 140 (2009) 64–69.
- [62] V.Y. Doluda, E.M. Sulman, V.G. Matveeva, M.G. Sulman, N.V. Lakina, A.I. Sidorov, P.M. Valetsky, L.M. Bronstein, Chem. Eng. J. 134 (2007) 256–261.
- [63] B.S. Furniss, A.J. Hannaford, V. Rogers, P.W.G. Smith, A.R. Tatchell, Vogel's Textbook of Practical Organic Chemistry Including Qualitative Organic Analysis, 1978.
- [64] J.J. Barbier, L. Oliviero, B. Renard, D. Duprez, Top. Catal. 33 (2005) 77–86.
- [65] L.S. Clesceri, A.E. Greenberg, R.R. Trusell, M.A. Franson, Standard Methods for the Examination of Water and Wastewater, 17th ed., American Public Health Association and American Water Works Association, Washington, 1989.
- [66] K.V. Klementiev, VIPER for Windows, Freeware, [www.desy.de/~klmn/viper.html](http://www.desy.de/~klmn/viper.html).
- [67] A. Gross, Theoretical Surface Science: A Microscopic Perspective, Springer, 2003.
- [68] F.E. Beamish, The Analytical Chemistry of the Noble Metals, Oxford, London, Edinburgh, New York, Toronto, Paris, Frankfurt, 1966.
- [69] J.C. Chaston, Platinum Met. Rev. 13 (1969) 28.